Materials Letters 190 (2017) 181–184

Contents lists available at ScienceDirect

Materials Letters

journal homepage: www.elsevier.com/locate/mlblue

Low temperature thermal oxidation towards hafnium-coated magnesium alloy for biomedical application

Dongfang Zhang [a], Zhengbing Qi [b], Binbin Wei [a], Zhoucheng Wang [a,*]

[a] College of Chemistry and Chemical Engineering, Xiamen University, Xiamen 361005, China
[b] School of Materials Science and Engineering, Xiamen University of Technology, Xiamen 361024, China

ARTICLE INFO

Article history:
Received 21 November 2016
Received in revised form 3 January 2017
Accepted 3 January 2017
Available online 4 January 2017

Keywords:
Magnesium alloy
Thermal oxidation
Surface
Corrosion

ABSTRACT

Low temperature thermal oxidation treatment is performed on the PVD (physical vapor deposition) hafnium-coated magnesium alloy. The results indicate that thin hafnium oxide film and new shallow grain boundaries were appeared on the coating surface. Surface oxidation and densification of the coating induced by the post treatment significantly decreased its susceptibility to corrosion. Moreover, the release of the residual stress produces a positive effect on suppressing the delaminating of the coating as magnesium is corroded. Consequently, the treated coating exhibits more positive corrosion potential, lower corrosion current density and higher polarization resistance than that of the untreated coating in Hanks' solution. Salt spray test further reveals that the post-treated hafnium coating can provide a longer-term and more efficient protection for magnesium alloy.

1. Introduction

Magnesium alloys are promising candidates as biocompatible implant materials in biomedical application considering their similar elastic modulus and compressive yield strength properties to natural bone [1–4]. Nevertheless, the poor resistance to surface degradation restricts their application [5–7]. Surface modification by PVD coatings has been convinced as a prospective solution [8,9]. However, for the PVD coatings, severe micro-galvanic corrosion on the coating/substrate interface and the growth-related coating defects (pinhole) should be taken into consideration [10,11].

Fortunately, the Hf exhibits the satisfactory protection due to the low potential difference to Mg alloy [12] and good biocompatibility [13]. In order to further increase the lifetime of PVD coatings, it is imperative to take measures to deal with the pinholes. Thermal oxidation treatment has been reported as an efficient way to improve the corrosion resistance of biomaterial [14]. This post-treatment was also attempted to apply on PVD coatings [15]. Although the previous works ascribe the improved corrosion resistance to surface oxidation, little information about the surface oxidation was available. The relationship between the anti-corrosion property and the evolution of microstructure induced by thermal oxidation was scarcely mentioned. Moreover, for Mg alloy (melting point ⩽650 °C), it is unacceptable to conduct the traditional thermal oxidation at high temperature [14–16]. In this study, low temperature thermal oxidation treatment was conducted on the PVD Hf-coated Mg alloy. Microstructure, composition and corrosion resistance of the post treated coatings were investigated to get insight into the relationships between them.

2. Experimental

The die-cast AZ91D Mg alloys were ground with emery paper #5000 grit and polished with diamond powder (particle size 2.5 μm), then ultrasonically degreased in acetone for 15 min. Prior to coating deposition, the substrates were ion cleaned for 5 min in order to remove surface oxide. The deposition parameters were described below: Ar flux 60 sccm, working pressure 0.35 Pa, Hf (99.9% purity) target DC power (Advanced Energy, U.S.) 250 W, substrate temperature 300 °C, bias voltage −100 V. Thermal oxidation treatment was carried out in a tube furnace at 300 °C for 5 h with a flow-through of air.

Crystal structure of the coatings was investigated by normal and glancing incidence X-ray diffraction (GIXRD) with Cu k_α radiation (Philips, Netherlands). The $\sin^2\psi$ method was employed to determine the biaxial residual stress, and Co radiation as X-ray source. X-ray photoelectron spectroscopy (XPS, PHI-Quantum 2000, US) was used to investigate the coating chemical bonding states. Surface morphologies were observed by scanning electron microscope (SEM, ZEISS SIGMA, Germany). The electrochemical

* Corresponding author.
E-mail address: zcwang@xmu.edu.cn (Z. Wang).

http://dx.doi.org/10.1016/j.matlet.2017.01.009
0167-577X/

tests were conducted in an electrolyte cell consisting of a working electrode (1 cm^2), counter electrode (platinum sheet) and reference electrode (SCE, saturated calomel electrode) using CHI660E (Chenhua, China) in Hanks' solution [17,18] at 37 °C. Potentiodynamic polarization test was carried out at a scan rate of 1 mV s^{-1}. The electrochemical impedance spectra were measured in a frequency range from 10 mHz to 100 kHz with AC perturbation of 10 mV. Neutral salt spray test (NSS) followed ASTM B117 was performed to evaluate the long-term protection to AZ91D. This test was performed for 48 h with a 5 wt% of NaCl solution at 35 ± 2 °C.

3. Results and discussion

Fig. 1a and b reveal the face-centered cubic structured Hf coatings (JCPDS No.05-0607) with the (002) preferred orientation. However, the (002) diffraction peak of the treated coating is shifted to a higher angle, indicating that the residual stress was relieved [19]. Generally, high residual stress existed in coating would eventually resulted in cracking or peeling [20]. Herein, the decreased stress value from −4.69 ± 0.38 to −3.85 ± 0.06 GPa by applying the post treatment helps to maintain the coating's integrity (Fig. 1c). Notably, the weak ($\bar{1}11$) peak belonging to HfO_2 (JCPDS No.34-0104) was observed in GIXRD pattern (Fig. 1d) of the treated Hf coating. XPS combined with Ar^+ sputtering etching (~20 nm depths) was used to investigate the hafnium oxide in detail. As shown in Fig. 1e and f, the untreated Hf coating shows two strong peaks with binding energies of 15.9 eV and 14.2 eV, corresponding to the Hf $4f_{7/2}$ and Hf $4f_{5/2}$ components of Hf, respectively [21]. Two weak peaks with binding energies of 19.1 eV and 17.5 eV on behalf of HfO_2 are also found in the same spectrum. However, the intensities of the peaks of 19.1 eV and 17.5 eV are significantly increased in the Hf 4f spectra of the treated coating. The result reveals that HfO_2 has become the dominant phase on the coating surface (~30 nm) after the post treatment.

The surface morphology of untreated Hf coating exhibits dense roof-like microstructure (Fig. 2a). As for the treated coating, numerous new grain boundaries (marked by the arrows) were observed on the old grains (Fig. 2b). The Pilling-Bedworth ratio of HfO_2 was about 1.62 [22]. Therefore, the presence of Hf oxide and new grain boundaries make the coating surface a higher density. Moreover, the expansion of old grains induced by the new grain boundaries produces a squeezing action on the old boundaries and seals the growth related pinholes of coating surface. Consequently, the probability of corrosion media penetrate through the treated coating is expected to be declined.

Fig. 3 presents the corrosion results of the AZ91D and the coated samples in Hanks' solution. The corrosion potential (E_{corr}) of the treated sample is more positive with the value of −0.96 V/SCE in comparison to the bare Mg alloy (−1.47 V/SCE) and the untreated sample (−1.37 V/SCE). The shift of the E_{corr} to a more positive value is mainly due to the formation of the thin HfO_2 film, which provides a barrier for corrosive media in the initial stage. The corrosion current density (i_{corr}) of the treated sample (0.78 μA·cm^{-2}) is significantly decreased compared with that of AZ91D (44.29 μA·cm^{-2}), and is also one order of magnitude lower than untreated sample (2.81 μA·cm^{-2}). The Nyquist plots are consistent with the polarization curves. The calculated polarization resistance of the treated sample (100.5 KΩ·cm^2) is 3 times higher than that of the untreated sample (31.5 KΩ·cm^2). As shown in Fig. 3c, after 48 h NSS, the untreated coating reveals a protection for AZ91D with several corrosion sites. However, no visible corrosion pits have been found on the treated coating's surface. The protection rating was significantly increased from 6 (area of corrosion 0.5–1.0%) to 9 (area of corrosion <0.1%) according to ASTM B537-70 [23].

Fig. 3d and e show the different corrosion types of the untreated and treated Hf-coated samples. Pitting corrosion and coating delaminating are observed on the untreated sample. Generally, high residual stress of PVD coating is prone to accelerate the prop-

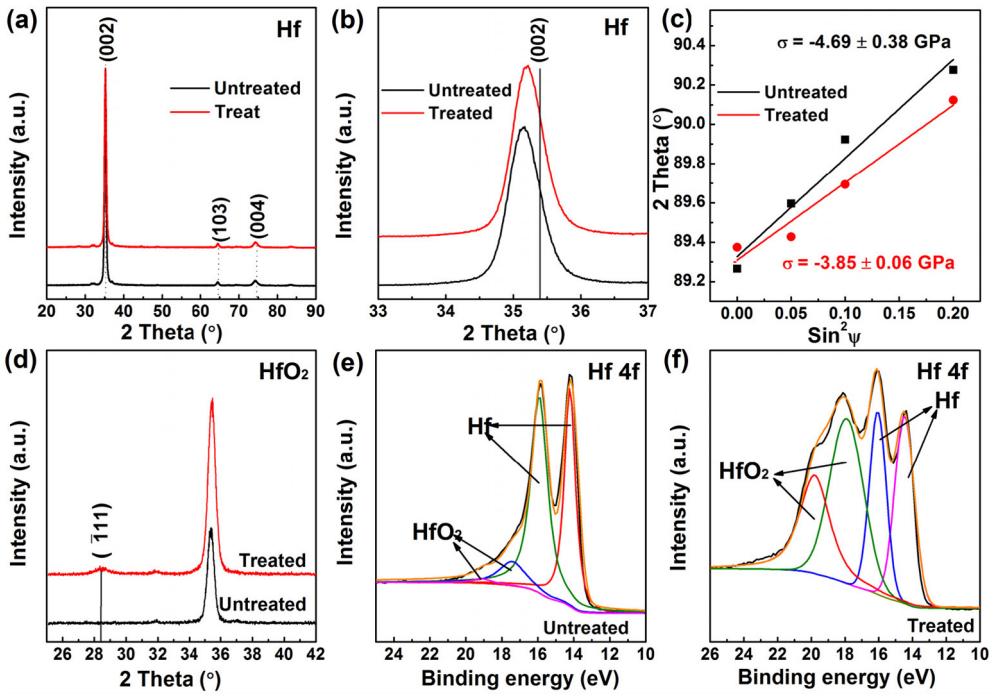

Fig. 1. (a) Normal XRD patterns, (b) maximum peaks of (a), (c) residual stress data, (d) GIXRD patterns, (e and f) the XPS spectra (depth ~20 nm) of the untreated and treated samples.